Chemiresistive Gas Sensing by Few-Layered Graphene

K. R. Nemade & S. A. Waghuley

Journal of Electronic Materials

ISSN 0361-5235
Volume 42
Number 10

Journal of Elec Materi (2013)
42:2857-2866
DOI 10.1007/s11664-013-2699-4

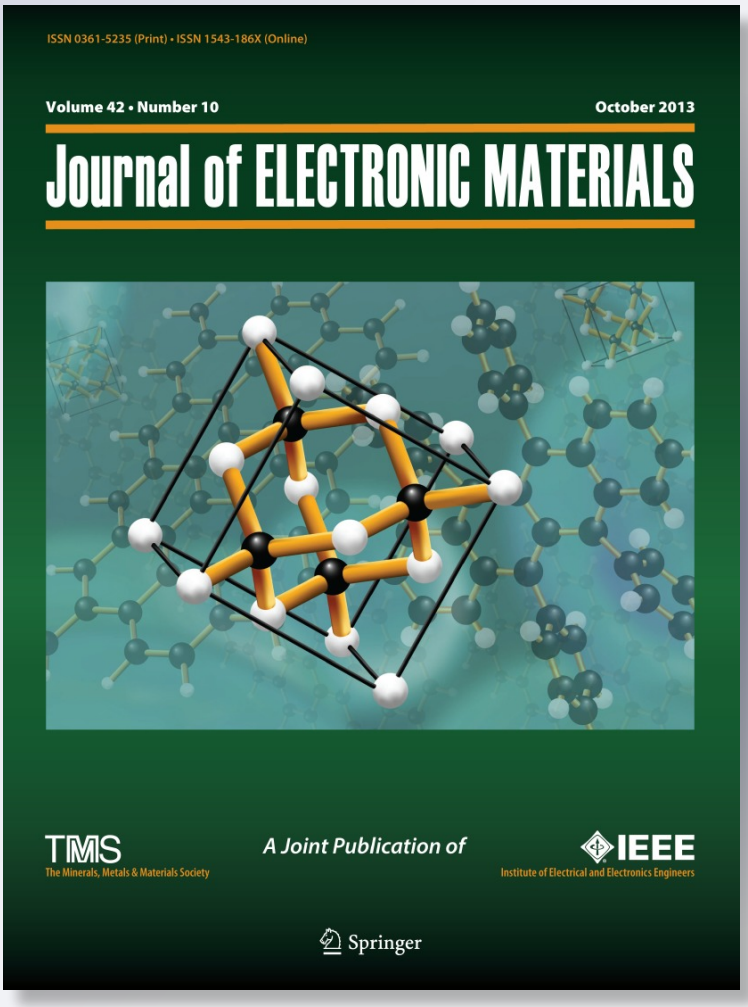

Springer

Journal of ELECTRONIC MATERIALS, Vol. 42, No. 10, 2013
DOI: 10.1007/s11664-013-2699-4

Chemiresistive Gas Sensing by Few-Layered Graphene

K.R. NEMADE[1] and S.A. WAGHULEY[1,2]

1.—Department of Physics, Sant Gadge Baba Amravati University, Amravati 444 602, India.
2.—e-mail: sandeepwaghuley@sgbau.ac.in

A chemiresistive gas sensor based on few-layered graphene (FLG) has been fabricated and evaluated for carbon dioxide (CO_2) and liquid petroleum gas (LPG) sensing. The electrochemical exfoliation method was used to synthesize FLG. The resulting sample of FLG was characterized by x-ray diffraction, Raman spectroscopy, atomic force microscopy, and transmission electron microscopy with selected-area diffraction. Ultraviolet–visible and fluorescence spectroscopy were employed to study the optical properties. Thermal behavior was analyzed through thermogravimetric–differential thermal analysis. The sensing response of the chemiresistor is defined as the ratio of resistance in gas to air at the stabilized resistance in air. The FLG chemiresistor exhibited good sensing response (3.83 for CO_2, 0.92 for LPG), response time (11 s for CO_2, 5 s for LPG), recovery time (14 s for CO_2, 18 s for LPG), and resolution limit (3 ppm for CO_2, 4 ppm for LPG), and excellent stability at room temperature. The gas sensing mechanism is discussed on the basis of marginal difference in Raman intensity and also by using defect chemistry through fluorescence measurements.

Key words: Few-layered graphene, carbon dioxide, liquid petroleum gas, defects

INTRODUCTION

Global warming has become a pressing environmental issue related to increasing atmospheric concentrations of greenhouse gases. Carbon dioxide (CO_2) is one of the most common gases evolved in combustion, also being a greenhouse gas.[1] CO_2 is a stable oxidizing gas, so its detection is challenging. In many fields, such as industrial emission control, household security, and vehicle emission control, monitoring of CO_2 is mandatory. Therefore, cost-effective and robust sensing materials are required for CO_2 detection. Correspondingly, liquid petroleum gas (LPG) has found useful application as a clean source of energy. However, its explosive nature means that reliable and efficient gas sensors that can detect even minute LPG concentrations are required.[2] Both of these gases are widely used for many domestic and industrial purposes; consequently their efficient and cost-effective sensing becomes even more essential.

In the light of this discussion, graphene is a potential gas-sensing material with enormous sensitivity. As defined by the International Union of Pure and Applied Chemistry, graphene is formed of 10 or fewer carbon atom layers, being divided into three major categories: (i) single-layer, (ii) 2-layer, and (iii) 3- to 10-layer graphene, known as monolayered, bilayered, and few-layered graphene (FLG), respectively. Yoon et al.[3] reported CO_2 sensing with FLG. Recent study has verified the detection of molecules by pristine graphene, attracting great research interest from both the scientific and engineering communities.[4] Many researchers have reported on gas-sensing applications of graphene.[5–8] Graphene is a highly promising material for use in terahertz devices, opening a new field of nanomaterial wave characteristics.[9–11] Graphene-based devices have low Johnson noise due to its low resistivity.[5]

Sensing responses can mainly be attributed to electron transfer between a material and chemisorbed

(Received March 13, 2013; accepted July 9, 2013; published online August 14, 2013)

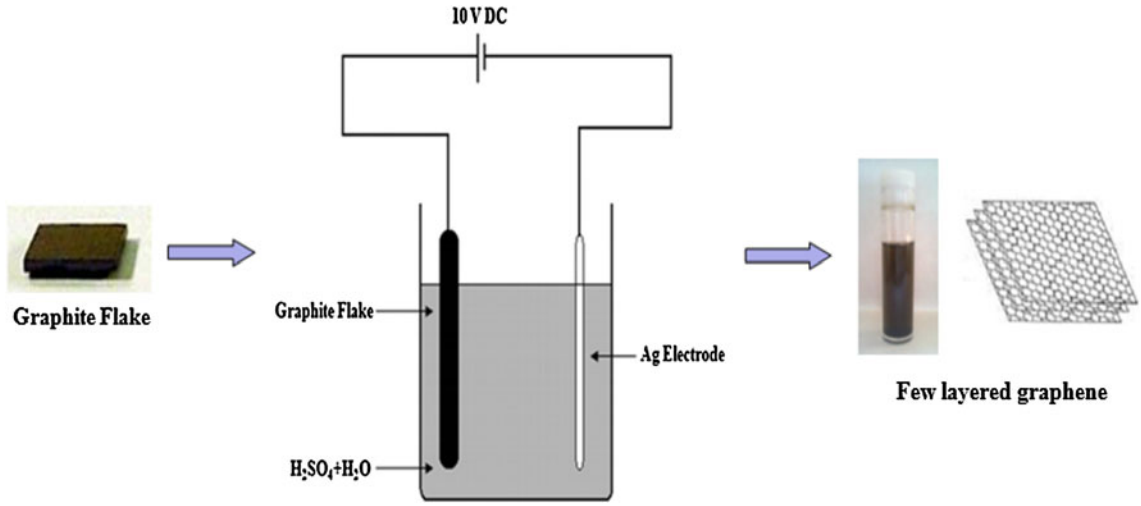

Fig. 1. Scheme of electrochemical exfoliation of graphite.

gaseous molecules. This is a redox-type reaction, leading to changes in the depletion layer of the grains that change the electrical resistance. There are many possible reactions for the change in electrical resistance; the most common reaction that leads to changes in the resistance/conductance is adsorption of gases on the surface of sensing materials. The transport properties of materials are mainly dependent on defect concentrations. Great emphasis should be placed on defect concentrations, as adsorption of gases and the sensing response are measured in terms of resistance.[12,13] Kaur et al.[14] reported sensing of H_2S gas at ppb levels and demonstrated that the sensing parameters are strongly affected by the concentration of defects. Lupan et al.[15] discussed the sensing mechanism for hydrogen gas, focusing on the role of defect chemistry. Hwang et al.[16] recently reported synthesis of graphene sheets from highly oriented pyrolytic graphite through mechanical cleavage in order to investigate its response in chemical vapor sensing.

In this work, we introduce a highly responsive chemiresistor based on FLG as a gas-sensing material for CO_2 and LPG. During literature survey, it was observed that researchers have reported synthesis of graphene by electrochemical exfoliation of graphite using platinum as a cathodic electrode. For the present investigation, we used a silver electrode for the electrochemical exfoliation process of graphite. This significantly reduced the preparation cost. The chemiresistor exhibits strong sensing response with fast response and recovery characteristics. The stability of the chemiresistor was found to be excellent. Some interesting accomplishments are reported.

EXPERIMENTAL PROCEDURES

FLG was synthesized from graphite flake using a modified electrochemical exfoliation method, in which a silver electrode was used as the cathodic electrode. For electrochemical exfoliation, graphite flake and the silver electrode were inserted into an ionic solution with separation of 5 cm. The ionic solution was prepared by taking 4.8 g sulfuric acid (99.99%; SD Fine) diluted in 100 mL double-distilled water. The process was carried out in a direct-current

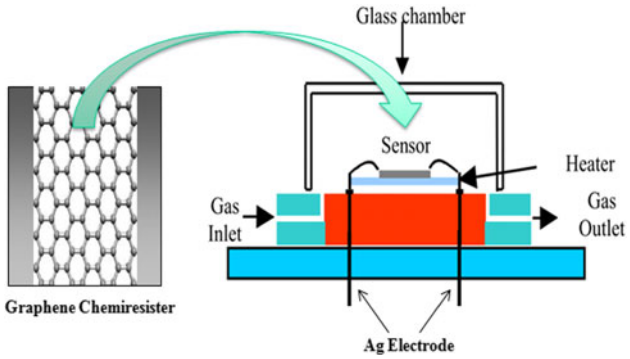

Fig. 2. Gas sensing setup.

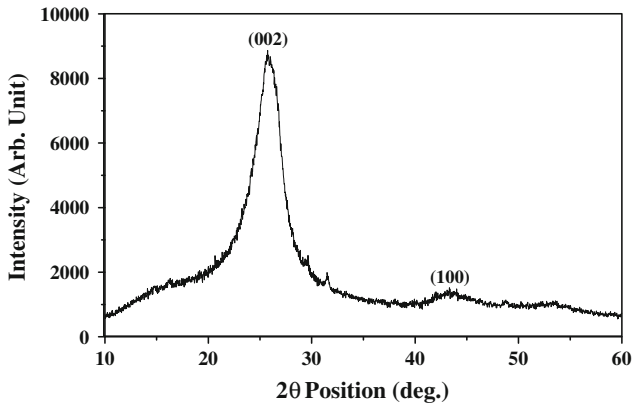

Fig. 3. XRD pattern of FLG.

(DC) bias (10 V) arrangement at room temperature (303 K).[17] Exfoliated FLG was collected through cellulose nitrate filter paper and washed with double-distilled water. The obtained sample was dried at 100°C for 2 h. Figure 1 shows the electrochemical exfoliation process of graphite.

The structural and phase purity of the as-prepared FLG were determined by x-ray diffraction (XRD, PW 1830; Philips). The morphology and few-layered structure were examined by atomic force microscopy (AFM, Webinar series; Bruker) and high-resolution transmission electron microscopy (HR-TEM, Tecnai F-30107; Philips) with selected-area diffraction pattern (SADP) analysis. Raman spectroscopy (RFS 27; Bruker; Raman spectrometer using a Nd:YAG laser excitation source at 514 nm) was employed to characterize the few-layered structure and quality of graphene. Optical characterization was done through ultraviolet–visible (UV–Vis; PerkinElmer) and fluorescence spectroscopy (FL spectrophotometer model F-7000; Hitachi). The thermal behavior of FLG was analyzed using thermogravimetric–differential thermal analysis (TG–DTA, DTG-60h; Shimadzu).

A chemiresistor is a type of variable-resistance sensor whose resistance changes in the presence of gases. For measurement of the gas-sensing response, dried FLG was dispersed with a temporary binder in a mixture of organic solvents to form a paste, prepared using a previously reported method.[18] For strong adhesion to a substrate, the ratio of FLG to binder was kept at 90:10 in formulating the paste. A thick film of FLG was deposited on a chemically cleaned glass substrate of 25 mm × 25 mm size by screen-printing, then dried at room temperature (303 K) for 24 h. Further heat treatment was applied to the film at 373 K for 3 h for evaporation of volatile organic compounds from the binder. The thickness of the chemiresistor was measured using a Digimatic (Japan) outside micrometer (series 293) having resolution of ±0.001 mm and found to be 7 μm. For surface resistance measurements, highly conducting silver paste was used to make ohmic contacts on adjacent sides of the film with electrode thickness of 12 μm, and then it was subjected to heating at 353 K for 15 min to dry the silver paint. The gap dimension of the chemiresistor was 21 mm × 25 mm. To check the gas-sensing response, the chemiresistor was loaded into a gas-sensing chamber. The temperature and humidity inside the chamber were precisely controlled. The sensing response was studied by using air as reference gas. The gas-sensing response (S) is defined as $S = |R_a - R_g|/R_a$, where R_a is the resistance in air (baseline resistance) and R_g represents the resistance in gas. During this experiment, the resistance of the chemiresistor was measured using the voltage drop method adopted by Waghuley et al.[18] The sensing parameters of the chemiresistor were analyzed at different concentrations (ppm) and temperatures. The gas concentration required inside the 5-L chamber was maintained by injecting a known volume of test gas using a gas-injection syringe of different volumes. The concentration inside the chamber was increased by adding a particular amount of gas; For example, 0.025 mL of gas added into the 5-L chamber was defined as 0.025 mL/5000 mL = $5/10^6$, i.e., 5 ppm. An outline of the gas-sensing system is shown in Fig. 2.

RESULTS AND DISCUSSION

Figure 3 shows the XRD pattern of the FLG, well supporting its structural and phase purity. There are two prominent peaks in the XRD pattern, (002) and (100), which are characteristic peaks of graphene. The sharp peak at $2\theta = 26.3°$ indicates a highly organized structure with interlayer spacing of 0.339 nm.[19] This is consistent with the layer spacing of typical graphite. The broad peak at $2\theta = 44.2°$ may be assigned to a lower degree of crystallization and the presence of some defects. This may be due to adsorption of oxygen molecules with amorphous carbon present on the FLG surface, as CO_2 molecules are known as a buffer gas.[19]

Atomic force microscopy and HR-TEM observations were employed to explore the surface morphology of the FLG. Raman spectroscopy was used to determine the number of graphene layers present in the stacked structure of graphene and its quality. Figure 4a shows an AFM image and height profile for the FLG. The average of the height distribution (H) of FLG was 1.7 nm. As the interlayer spacing between two graphene sheets (d) is 0.339 nm ($H/d = 5.01$), the stacked graphene was five-layered. Figure 4b shows the Raman spectrum of the FLG. The most important Raman features of FLG are the D band (~1300 cm^{-1}), G band (1580 cm^{-1}), and 2D band (~2720 cm^{-1}). The D band is associated with the density of defects. The intensity of the D band is directly proportional to the concentration of defects. This band is the result of a one-phonon lattice vibrational process, which is typically very weak in graphene. In our case, the D band is less notably than the G and 2D bands. The G band is assigned to in-plane vibration of sp^2 carbon atoms.[20] The 2D band originates from a two-phonon double-resonance process.[21] The intensity ratio of the G to 2D band is related to the number of graphene layers.[22] The relation between the number of graphene layers (N) and the intensity ratio of the G to 2D band is $N = (I_G/I_{2D})$, where I_G is the intensity of the G band and I_{2D} is the intensity of the 2D band. The value of N is less than one for mono- and bilayered graphene.[23] This value ranges from 1.3 to 2.4 for 5 to 10 layers of graphene.[24] In the present work, the value of N was found to be 1.64, which lies between 1.3 and 2.4, reflecting the few-layered structure of the graphene. This confirms that the synthesized graphene was few-layered. The full-width at half-maximum of the 2D peak is 80 cm^{-1}, also reflecting

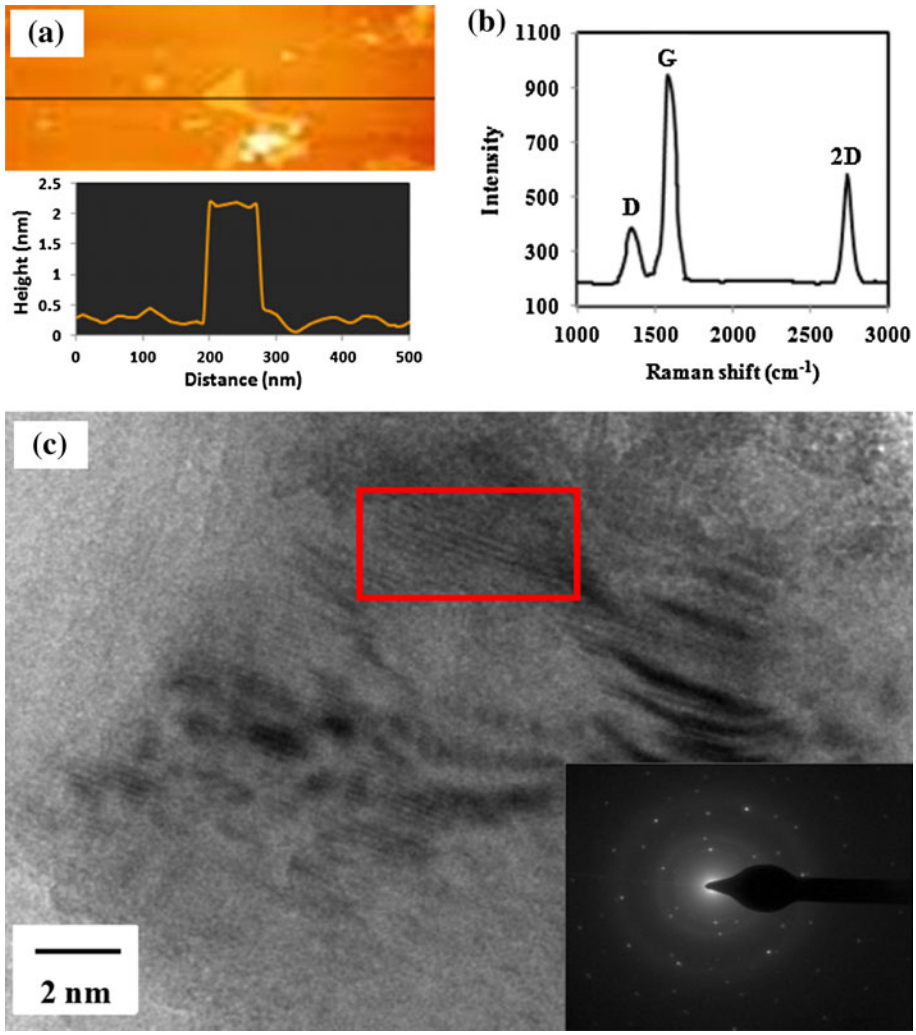

Fig. 4. (a) AFM image with height distribution of FLG. (b) Raman spectrum of FLG and (c) HR-TEM image showing the layered structure of the graphene. The inset shows a SADP image of the FLG.

the few-layered graphene structure.[25] The few-layered structure of graphene can be visualized directly by HR-TEM, as shown in Fig. 4c (highlighted in a red box). The inset of Fig. 4c shows a SADP image of the FLG, agreeing with the results obtained from XRD analysis. The rings in the diffraction pattern match the principal (002) and (100) peaks of graphene. The clear SADP image is due to the layered structure of graphene, showing the hexagonal symmetry.[23]

UV–Vis spectroscopy provides a tentative idea about the layered structure of the graphene. The optical transmission spectrum of FLG is shown in Fig. 5.

The intense absorption at 268 nm may be exhibited due to the few-layered structure of graphene. This is assigned to π–π^* transitions of C–C bonds.[26] The linear increase in the ultraviolet region around 268 nm and nearly flat transmission on the order of

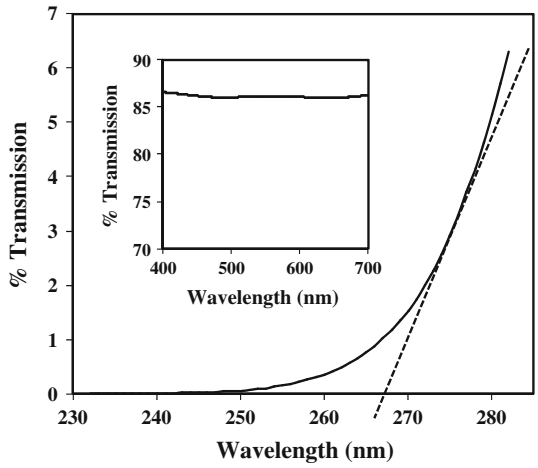

Fig. 5. Transmission spectrum of FLG in the UV and visible region (inset).

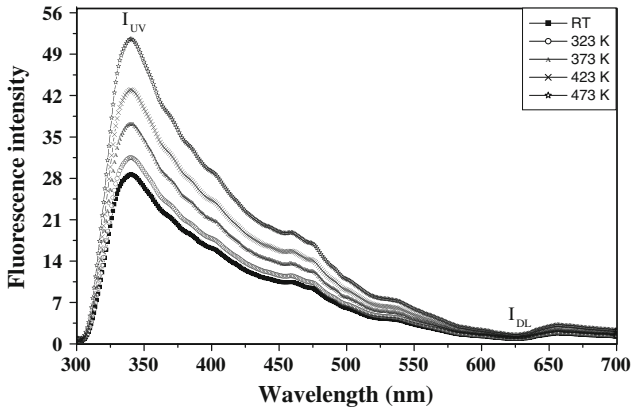

Fig. 6. Fluorescence measurements of FLG against sintering temperature with excitation at 254 nm.

Table I. I_{UV}, I_{DL}, and I_{UV}/I_{DL} ratio values for FLG for different sintering temperatures

Temperature (K)	I_{UV}	I_{DL}	I_{UV}/I_{DL}
303	28.20	1.5	18.8
323	31.38	1.53	20.50
373	36.66	1.56	23.5
423	42.30	1.63	25.95
473	51.35	1.67	30.74

86% in the visible region (400 nm to 700 nm) may be assigned to six-layered graphene.[23,26,27] Analyzing and combining the results from AFM, Raman, HR-TEM, SADP, and UV–Vis spectroscopy, it can be concluded that five or six layers of graphene are present in the stacked graphene.

Fluorescence spectroscopy can assess the concentration of defects in a material, which is relevant as the sensing parameters are strongly affected by the defect concentration.[28,29] To calculate the defect concentration, fluorescence measurements were carried out from 300 nm to 700 nm, as shown in Fig. 6. The intensity ratio of ultraviolet (I_{UV}) to visible deep levels (I_{DL}) is a measure of the defect concentration.[15] As shown in the figure, the (I_{UV}/I_{DL}) ratio was found to increase with the sintering temperature. In the present work, the FLG emitted intense blue luminescence under irradiation at 254 nm. The peak value of the emission was observed at 343 nm. The I_{UV}, I_{DL}, and (I_{UV}/I_{DL}) ratio values for the FLG are listed in Table I against sintering temperature. This shows that defects are present on the surface of the FLG and increase with the sintering temperature.

Figure 7 shows the TG–DTA results for the FLG, to show the thermal stability during heat treatment. The TG–DTA analysis was carried out from room temperature to 775 K in nitrogen atmosphere.

There are two major mass change steps with increasing temperature. According to the TGA percentage curve, the sample shows a sharp weight loss up to 373 K, and the DTA curve shows an endothermic peak at 342 K, corresponding to evaporation of absorbed water. The total mass loss from room temperature to 450 K was about 15.22%. The DTA curve shows another exothermic peak at 740 K, which may correspond to generation of disorder defects.

Figure 8 shows the dependence of the sensing response of the FLG chemiresistor on the concentration of CO_2 and LPG at room temperature. The baseline resistance for the FLG chemiresistor is 2.236×10^6 Ω. In this experiment, a known amount of gas was inserted into the chamber, which was initially filled with air. Upon exposure to CO_2 (an oxidizing gas), the resistance of the FLG chemiresistor increased. However, the resistance of the chemiresistor decreased when it was exposed to LPG (a reducing gas). This confirms that FLG exhibits *n*-type characteristics.[30] The sensing response of the chemiresistor was found to vary linearly with the concentration of CO_2 gas. This linear relationship between the response and the CO_2 gas concentration suggests that the chemiresistor response exhibits a good dependence on the gas concentration. Saturation was observed for LPG above 75 ppm. This may indicate the optimum detection limit for LPG.

To determine the interaction between oxygen-adsorbed FLG and CO_2 or LPG gas, Raman spectroscopy was performed. Figure 9 depicts the Raman spectra of FLG in CO_2 and LPG environments, acquired after testing the sensing response of FLG towards CO_2 and LPG at room temperature. The intensities of almost all the peaks shown in the Raman spectrum were significantly affected. Among these bands, the D band is strongly affected. This may be due to gas molecules forming surface species such as surface carbonate and water, which affect the one-phonon lattice vibration process.

This observation can also be explained based on the surface reaction between adsorbed oxygen ions and the gas molecules. Oxygen may be either adsorbed as uncharged molecules or chemisorbed as charged species on the film surface.[31] For adsorbed oxygen ions, the interactions are

$$O_2(\text{gas}) \rightarrow O_2(\text{ads})$$
$$O_2(\text{ads}) + e^- \rightarrow O_2^-(\text{ads})$$
$$O_2^-(\text{ads}) + e^- \rightarrow 2O^-(\text{ads})$$

A great number of oxygen ions on the surface creates a higher potential barrier; therefore, the resistance of the chemiresistor increases.[32] The CO_2 gas detection mechanism of the FLG chemiresistor is based on the reaction that occurs between adsorbed oxygen and CO_2 gas molecules. CO_2 is a strong oxidizer gas with electron-withdrawing power. When the chemiresistor is exposed to CO_2

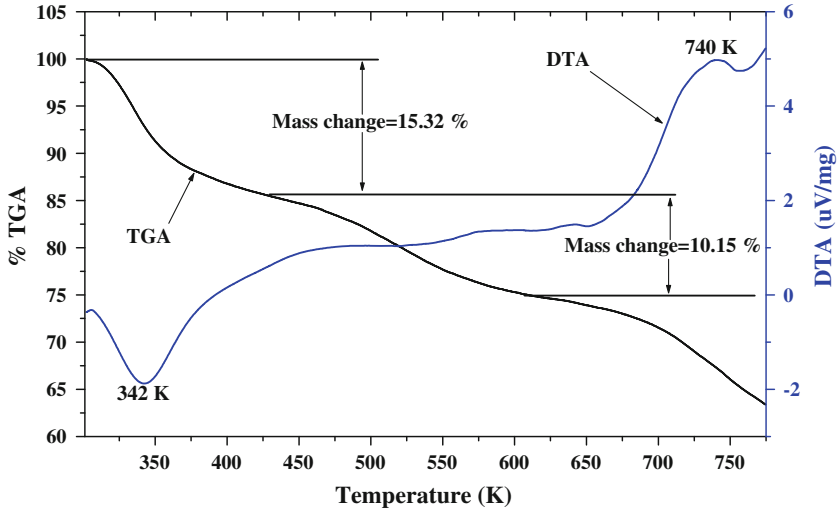

Fig. 7. TG–DTA curves of FLG.

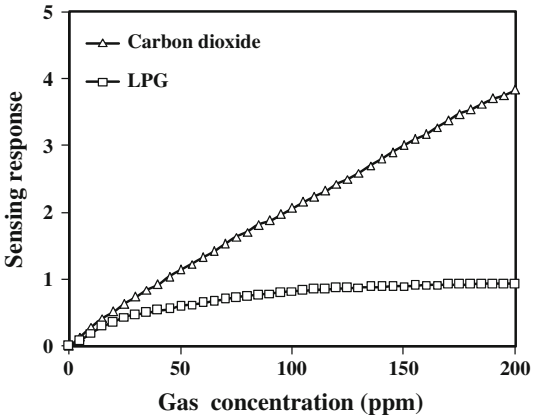

Fig. 8. Sensing response of the chemiresistor towards CO_2 and LPG at room temperature.

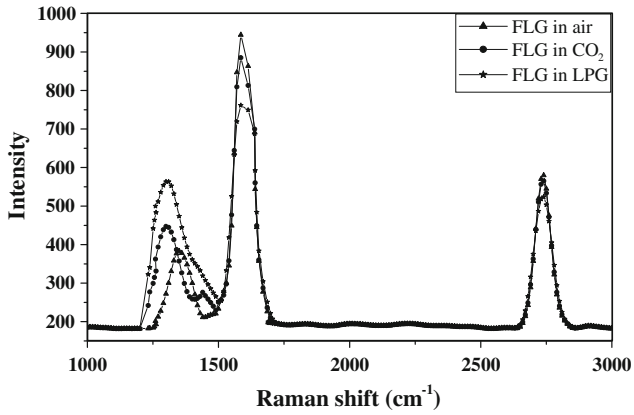

Fig. 9. Raman spectra of FLG in CO_2 and LPG environments.

gas, the gas is chemisorbed onto bridging oxygen atoms with the formation of a surface carbonate and increase in the resistance of the chemiresistor.[33] The interactions between CO_2 and adsorbed oxygen ions are

$$CO_2 + 2O^-(\text{ads}) \rightarrow CO_3^{2-}$$
$$CO_2 + O^-(\text{ads}) \rightarrow CO_3^-$$

LPG is composed of CH_4, C_3H_8, C_4H_{10}, etc., and these molecules are reducing species. When the chemiresistor is exposed to LPG, the LPG interacts with adsorbed oxygen ions to form H_2O and CO_2. The interactions between LPG and adsorbed oxygen ions are[34]

$$C_nH_{2n+2} + 2O^-(\text{ads}) \rightarrow H_2O + C_nH_{2n} : O + e^-$$
$$C_nH_{2n} : O + O^-(\text{ads}) \rightarrow CO_2 + H_2O + e^-$$

Figure 10 shows the variation of the gas-sensing responses of the FLG chemiresistor and the I_{UV}/I_{DL} ratio (obtained from fluorescence measurements) as a function of temperature for constant concentration of CO_2 (30 ppm, 40 ppm, and 50 ppm). It is noticeable that excellent correlation exists between the I_{UV}/I_{DL} ratio and the gas-sensing response with temperature.

Figure 11 shows the variation of the gas-sensing responses and I_{UV}/I_{DL} ratio as a function of temperature for constant concentration of LPG (30 ppm, 40 ppm, and 50 ppm). Here also, excellent correlation is observed between the I_{UV}/I_{DL} ratio and the gas-sensing response with temperature.

The highest value of the sensing response was found at 423 K for CO_2 and 398 K for LPG for 30 ppm, 40 ppm, and 50 ppm. Therefore, for CO_2 gas detection, the operating temperature of the chemiresistor can be 423 K, and 398 K for LPG. This strong sensing response can be attributed to an

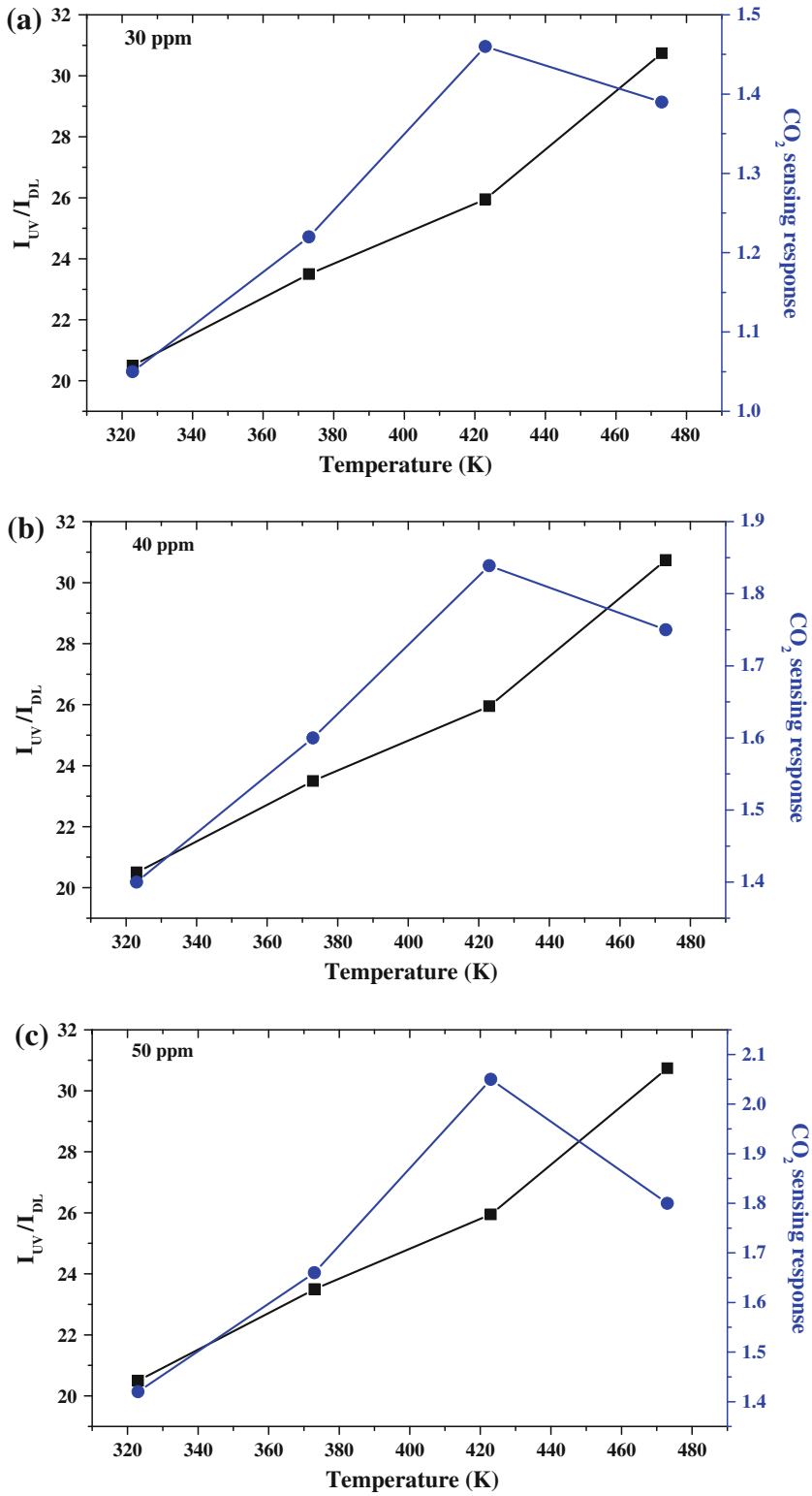

Fig. 10. Variation of the I_{UV}/I_{DL} ratio and CO_2 sensing response as a function of temperature for (a) 30 ppm, (b) 40 ppm, and (c) 50 ppm.

increase in the concentration of defects. The most probable defects in graphene are hexagonal defects in the form of oxygen vacancies.[35,36] As the temperature increases, the defect concentration also increases and emerges onto the surface of the chemiresistor. These defects in the form of vacant sites are available for chemisorption of atmospheric oxygen.[37] The greater the number of defects, the more oxygen will be chemisorbed. This results in enhancement of the sensing response. However, in

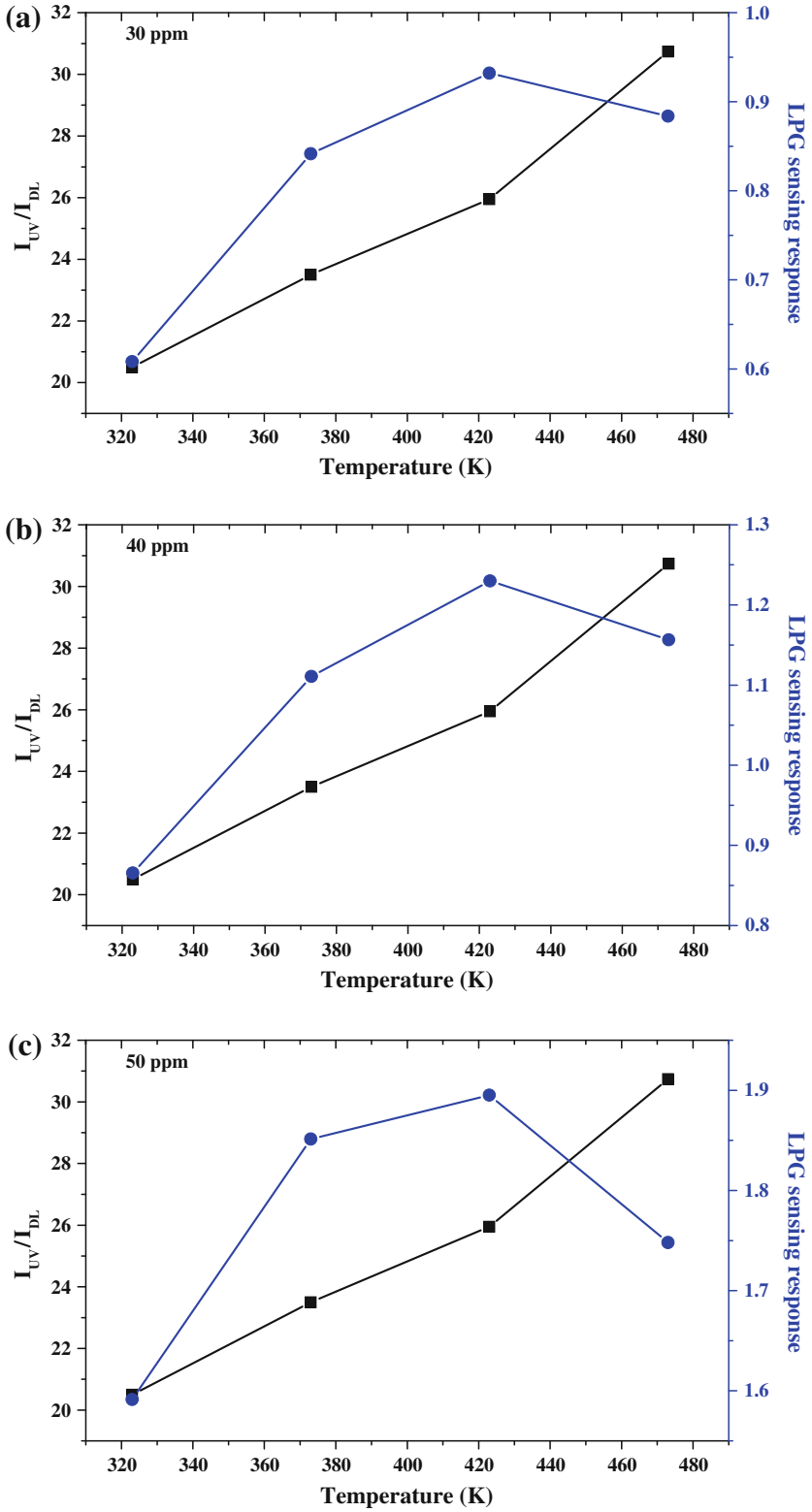

Fig. 11. Variation of the I_{UV}/I_{DL} ratio and LPG sensing response as a function of temperature for (a) 30 ppm, (b) 40 ppm, and (c) 50 ppm.

both cases, the response decreases above certain higher temperatures, as the absorbed oxygen is desorbed from the surface of the chemiresistor. This is one of the possible explanations for the lowering of the response at high temperatures. This result is well consistent with observations by Kapase et al.[31]

Figure 12a shows the transient response characteristics of the chemiresistor for CO_2 and LPG,

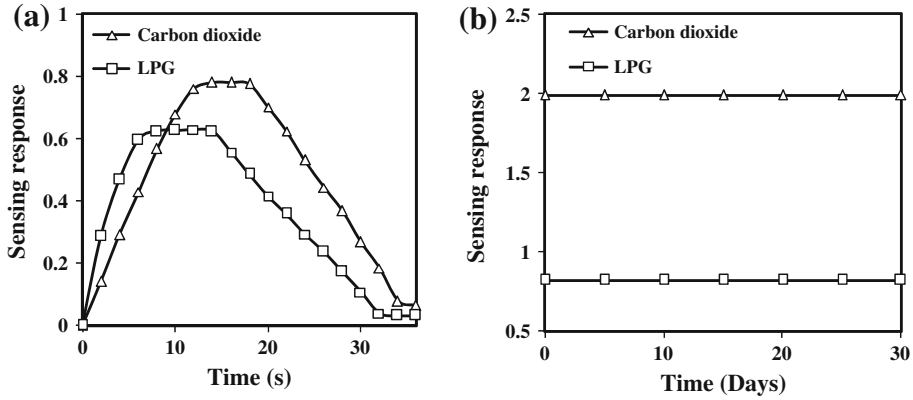

Fig. 12. (a) Transient and (b) stability response characteristics of FLG to 100 ppm CO_2 gas and LPG at room temperature.

measured to determine the response and recovery times at room temperature for 100 ppm. The response time of the chemiresistor can be defined as the time required for its resistance to change from its initial value to 90% of its highest value, whereas the recovery time of the chemiresistor can be defined as the time taken for its resistance to reduce by 90% from its highest value. In this measurement, gas was inserted into the chamber and the resistance of the chemiresistor was measured. The response time was found to be 11 s for CO_2 gas and 5 s for LPG. To measure the recovery time, the sample was exposed to air. The recovery time was found to be 14 s for CO_2 gas and 18 s for LPG. This fast response characteristic may be attributed to the fast interaction of gas molecules with the FLG surface, whereas the slow recovery can be attributed to strong bonding of the gas molecules to the absorbed oxygen, requiring a longer time for the annihilation process. To check the stability of the chemiresistor, its response towards 100 ppm of CO_2 and LPG at room temperature was measured for 30 days at intervals of 5 days after the first measurement. The results are illustrated in Fig. 12b. The chemiresistor showed a nearly constant response to CO_2 gas and LPG, indicating good stability of the chemiresistor. This shows that the graphene chemiresistor possesses good stability.

The resolution limit is the lowest concentration difference that can be distinguished by the chemiresistor.[38] The resistance of the chemiresistor in air was 2.236×10^6 Ω. The resolution limit characteristic was measured by injecting a known volume of gas into the chamber. A sharp change from the resistance value in air for a particular gas concentration was considered to indicate the resolution limit of the chemiresistor. The resolution limit results are presented in Tables II and III for CO_2 and LPG, respectively.

The resolution limit value was found to be 3 ppm and 4 ppm for CO_2 and LPG, respectively. It was observed that absorption of even minute concentrations (ppm) of gas could change the resistance of the chemiresistor.

Table II. Resolution limit of the chemiresistor for CO_2 gas

Concentration of CO_2 Gas (ppm)	Resistance of Chemiresistor (Ω)
0 (air)	2.236×10^6
1	2.236×10^6
2	2.236×10^6
3	2.417×10^6

Table III. Resolution limit of the chemiresistor for LPG

Concentration of LPG (ppm)	Resistance of Chemiresistor (Ω)
0 (air)	2.236×10^6
1	2.236×10^6
2	2.236×10^6
3	2.236×10^6
4	2.317×10^6

In the present case, the strongest sensing response was found to be on the order of 3.83 for CO_2 at 200 ppm, which is better than reported in Refs. 3,39. The operating temperature for CO_2 gas detection is 423 K, which is also much lower than in Ref. 40. The low operating temperature (398 K) and infinitesimal resolution limit (4 ppm) for LPG sensing are the most attractive features of the present work, as operation of LPG chemiresistors at high temperatures is difficult due to the explosive nature of the gas. The good sensing response (0.92), lower operating temperature (398 K), fast response time (5 s) and recovery time (18 s), and lower resolution limit (4 ppm) are adequate for use as a practical LPG sensor. The low operating temperatures for

both investigated gases significantly reduce the operating cost.

CONCLUSIONS

We have demonstrated a chemiresistive gas-sensing application of FLG synthesized by electrochemical exfoliation using silver as a cathodic electrode. The phase composition as analyzed by XRD showed the formation of FLG. Raman spectroscopy results confirmed that the FLG surface possesses fewer defects and a layered structure. The layered structure was also confirmed by AFM and HR-TEM. The FLG chemiresistor exhibited a good sensing response for CO_2 and LPG gases at room temperature as well as at relatively low operating temperatures. The sensing response showed a good dependence on the concentration of defects. The chemiresistor realized detection of CO_2 and LPG with rapid response and recovery. The chemiresistor was found to exhibit good stability for CO_2 and LPG sensing. The chemiresistor exhibited low resolution limit values for both investigated gases. Such detection of lower concentrations can be useful for practical applications. The described FLG chemiresistor may be a good candidate for practical use in CO_2 and LPG detection based on the good characteristics mentioned.

ACKNOWLEDGEMENTS

The authors are very grateful to the Head of the Department of Physics, Sant Gadge Baba Amravati University, Amravati, India and the Head of the Department of Chemical Science, North Maharashtra University, Jalgaon, India for providing necessary facilities.

REFERENCES

1. S.A. Waghuley, R.S. Bobade, A.V. Kohle, G.G. Muley, S.S. Yawale, F.C. Raghuvanshi, B.H. Pawar, and S.P. Yawale, *Adv. Mater. Rapid Commun.* 4, 97 (2010).
2. D. Haridas, V. Gupta, and K. Sreenivas, *Bull. Mater. Sci.* 31, 1 (2008).
3. H.J. Yoon, D.H. Jun, J.H. Yang, Z. Zhou, S.S. Yang, and M.M. Cheng, *Sens. Actuators B* 157, 310 (2011).
4. K.R. Ratinac, W. Yang, S.P. Ringer, and F. Braet, *Environ. Sci. Technol.* 44, 1167 (2010).
5. F. Schedin, A.K. Geim, S.V. Morozov, E.W. Hill, P. Blake, M.I. Katsnelson, and K.S. Novoselov, *Nat. Mater.* 6, 652 (2007).
6. H.Y. Jeong, D.S. Lee, H.K. Choi, D.H. Lee, J.E. Kim, J.Y. Lee, W.J. Lee, S.O. Kim, and S. Choi, *Appl. Phys. Lett.* 96, 213105 (2010).
7. G. Ko, H.Y. Kim, J. Ahn, Y.M. Park, K.Y. Lee, and J. Kim, *Curr. Appl. Phys.* 10, 1002–1004 (2010).
8. Y. Dan, Y. Lu, N.J. Kybert, Z. Luo, and A.T.C. Johnson, *Nano Lett.* 9, 1472–1475 (2009).
9. J.S. Bunch, A.M. Zande, S.S. Verbridge, I.W. Frank, D.M. Tanenbaum, J.M. Parpia, H.G. Craighead, and P.L. McEuen, *Science* 315, 490 (2007).
10. S. Stankovich, D.A. Dikin, G.H.B. Dommett, K.M. Kohlhaas, E.J. Zimney, E.A. Stach, R.D. Piner, S.T. Nguyen, and R.S. Ruoff, *Nature* 442, 282 (2006).
11. B. Aras and Q. Wang, *Comput. Mater. Sci.* 60, 245 (2012).
12. Y. Zhang, J.Q. Xu, Q. Xiang, H. Li, Q.Y. Pan, and P.C. Xu, *J. Phys. Chem. C* 113, 3430 (2009).
13. T. Gao and T.H. Wang, *Appl. Phys. A* 80, 1451 (2005).
14. M. Kaur, N. Jain, K. Sharma, S. Bhattacharya, M. Roy, A.K. Tyagi, S.K. Gupta, and J.V. Yakhmi, *Sens. Actuators B* 133, 456 (2008).
15. O. Lupan, V.V. Ursaki, G. Chai, L. Chow, G.A. Emelchenko, I.M. Tiginyanu, A.N. Gruzintsev, and A.N. Redkin, *Sens. Actuators B* 144, 56 (2010).
16. S. Hwang, J. Lim, H. Park, W.K. Kim, D. Kim, I.S. Song, J.H. Kim, S. Lee, D.H. Woo, and S.C. Jun, *Curr. Appl. Phys.* 12, 1017 (2012).
17. C. Su, A. Lu, Y. Xu, F. Chen, A. Khlobystov, and L. Li, *ACS Nano* 5, 2332 (2011).
18. S.A. Waghuley, S.M. Yenorkar, S.S. Yawale, and S.P. Yawale, *Sens. Actuators B* 128, 366 (2008).
19. Y. Wu, B. Wang, Y. Ma, Y. Huang, N. Li, F. Zhang, and Y. Chen, *Nano Res.* 3, 661 (2010).
20. Z. Ni, Y. Wang, T. Yu, and Z. Shen, *Nano Res.* 1, 273 (2008).
21. C. Thomsen and S. Reich, *Phys. Rev. Lett.* 85, 5214 (2000).
22. A. Reina, X. Jia, J. Ho, D. Nezich, H. Son, V. Bulovic, M.S. Dresselhaus, and J. Kong, *Nano Lett.* 9, 30 (2009).
23. N.K. Memon, S.D. Tse, J.F. Al-Sharab, H. Yamaguchi, A.B. Goncalves, B.H. Kear, Y. Jaluria, E.Y. Andrei, and M. Chhowalla, *Carbon* 49, 5064 (2011).
24. A.W. Robertson and J.H. Warner, *Nano Lett.* 11, 1182 (2011).
25. S. Bhaviripudi, X. Jia, M.S. Dresselhaus, and J. Kong, *Nano Lett.* 10, 4128 (2010).
26. T. Kuila, S. Bose, A.K. Mishra, P. Khanra, N.H. Kim, and J.H. Lee, *Prog. Mater. Sci.* 57, 1061 (2012).
27. Z. Sun, Z. Yan, J. Yao, E. Beitler, Y. Zhu, and J.M. Tour, *Nature* 468, 549 (2010).
28. P.C. Chang, Z. Fan, D. Wang, W.Y. Tseng, W.A. Chiou, J. Hong, and J.G. Lu, *Chem. Mater.* 16, 5133 (2004).
29. R. Schaub, E. Wahlstrom, A. Ronnaus, E. Laegsgaard, I. Stensgaard, and F. Besen-Bacher, *Science* 299, 377 (2003).
30. J. Wang, Y. Kwak, I. Lee, S. Maeng, and G. Kim, *Carbon* 50, 4060 (2012).
31. V.D. Kapase, S.A. Ghosh, G.N. Chaudhari, and F.C. Raghuwanshi, *Talanta* 76, 610 (2008).
32. S.R. Morisson, *Sens. Actuators B* 12, 425 (1987).
33. S.A. Waghuley, S.M. Yenorkar, S.S. Yawale, and S.P. Yawale, *Sens. Transducers* 79, 1180 (2007).
34. L.K. Bangal, J.Y. Patil, I.S. Mulla, and S.S. Suryavanshi, *Ceram. Int.* 38, 4835 (2012).
35. J. Dai and J. Yuan, *Phys. Rev. B* 81, 165414 (2010).
36. O.V. Yazyev and L. Helm, *Phys. Rev. B* 75, 125408 (2007).
37. S. Pati, S.B. Majumder, and P. Banerji, *J. Alloys Compd.* 541, 376 (2012).
38. V.E. Bochenkov and G.B. Sergeev, *Am. Sci. Publ.* 3, 31 (2010).
39. P. Matheswaran, R. Sathyamoorthy, and K. Asokan, *Sens. Actuators B* 177, 8 (2013).
40. M. Casas-Cabanas, A.V. Chadwick, M.R. Palacín, and C.R. Michel, *Sens. Actuators B* 157, 380 (2011).